Multi-axial fatigue behaviour of high-strength steel obtained by additive manufacturing: effects of defects and microstructure

January 17, 2023

JDD CETIM 2023 – Session 1: Fabrication Additive

Author: **Sai Sreenivas PENKULINTI**, Doctorant (2022-2025) – I2M Bordeaux, ENSAM

Directeur de thèse: **Nicolas SAINTIER**, Professor at ENSAM, I2M - DuMAS dept.

Co-encadrants: **Matthieu BONNERIC**, Enseignant-Chercheur at ENSAM, I2M - DuMAS dept.

Thierry PALIN-LUC, Professor at ENSAM, Director of I2M Bordeaux.

Benoit VERQUIN, Additive Manufacturing Expert – CETIM.

Fabien LEFEBVRE, Fatigue Expert – CETIM.

Outline

- ❑ Motivation
- ❑ Thesis objectives
- ❑ Literature Review
- ❑ Microstructure and defect population control
- ❑ Statistical analysis of defects
- ❑ Conclusions

Motivation

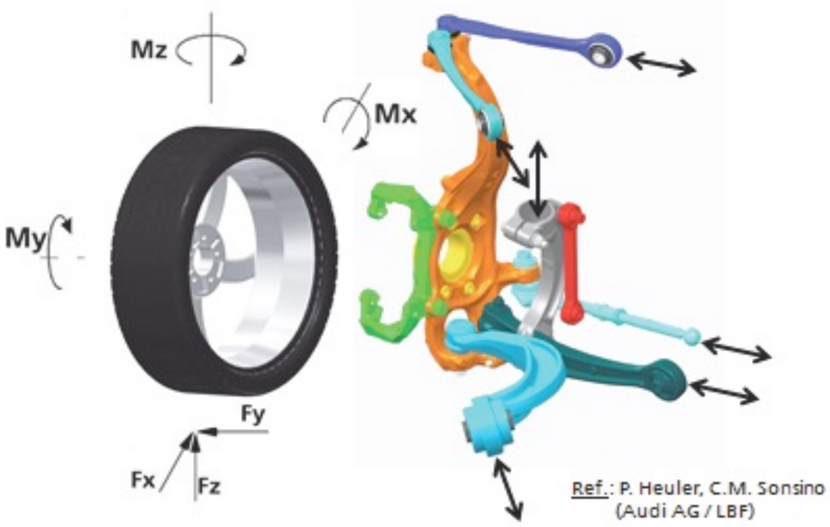

Multiaxial loads acting on wheel and steering knuckle *[C.M. Sonsino et al., Frattura ed Integrità Strutturale, 2016]*

Challenges

Lab to Industrial application

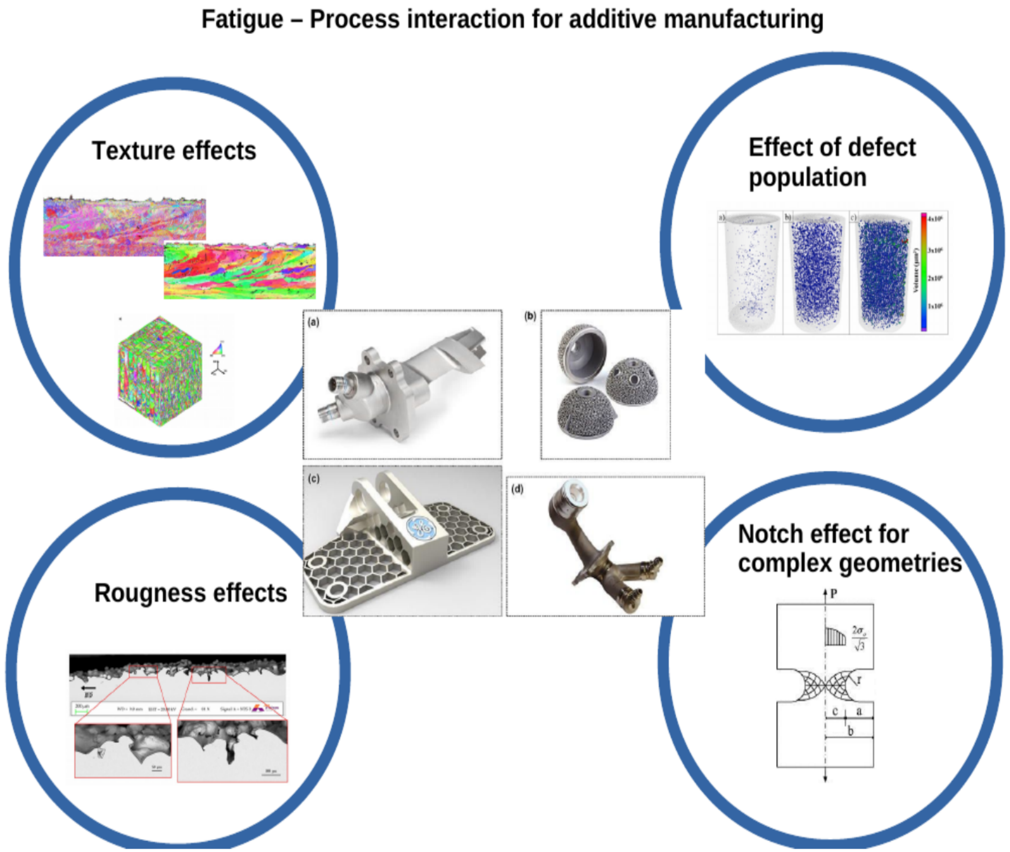

Thesis objectives

1. Experimental fatigue campaign

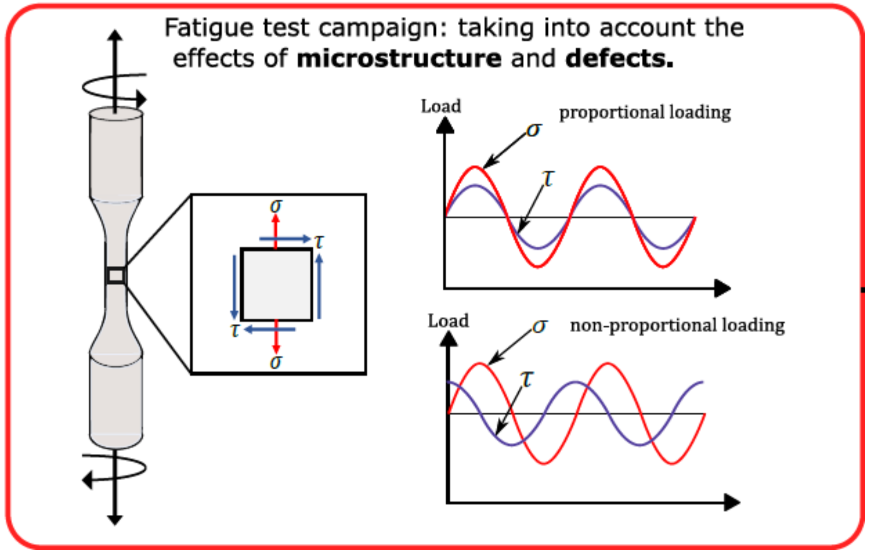

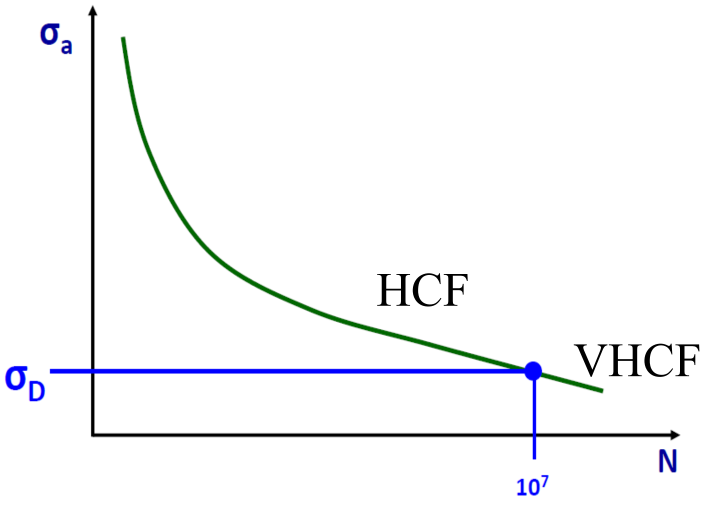

2. Identification of damage mechanisms

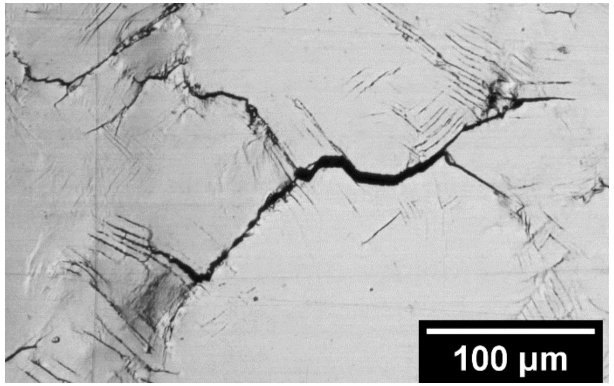

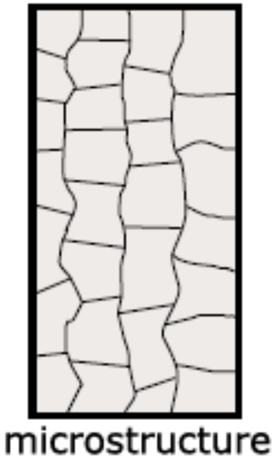

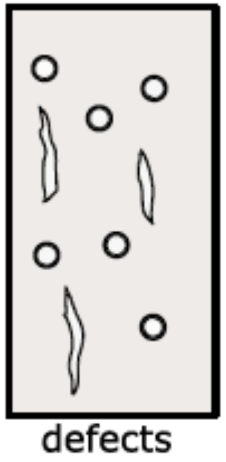

3. Numerical approach

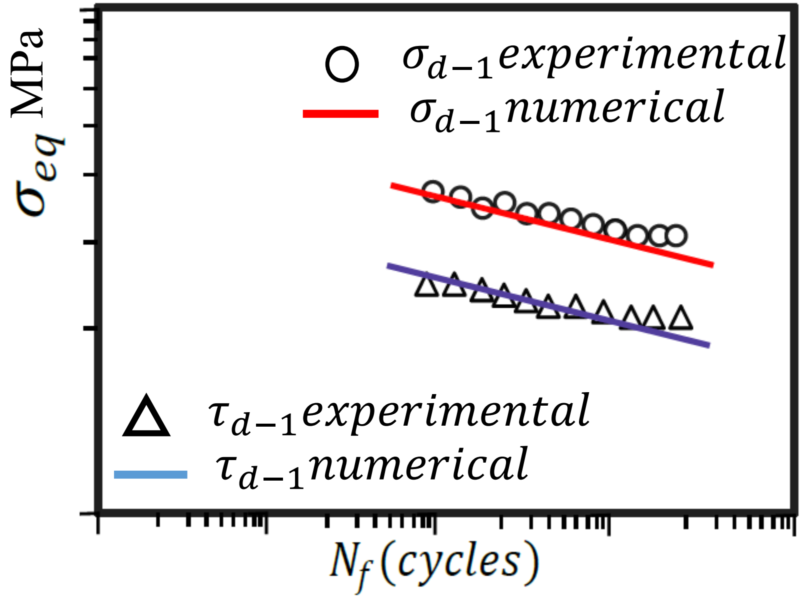

Literature Review

Formation of defects

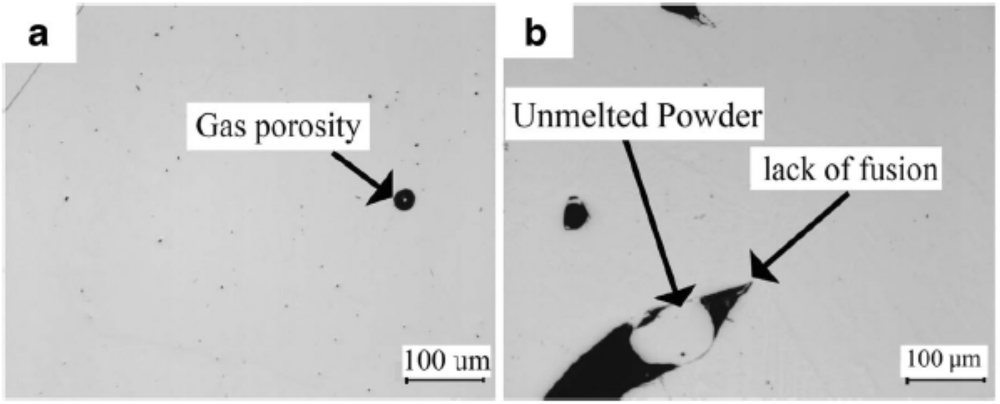

Metallographic observation of **Inconel 718**. *[P.Karimi et al.,Intl Adv Manuf Tech, 2018]*

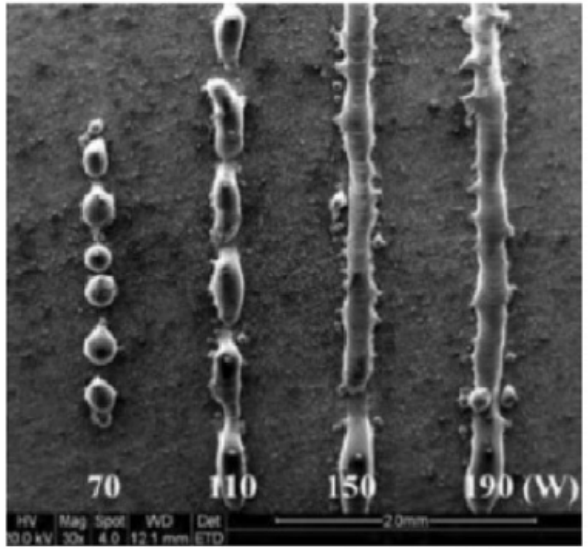

Balling phenomenon observed on SS 316L. *[Bourell, David et al., 2017, In: CIRP Annals - Manufacturing Technology]*

$$VED = \frac{P}{vht}\ J/mm^3$$

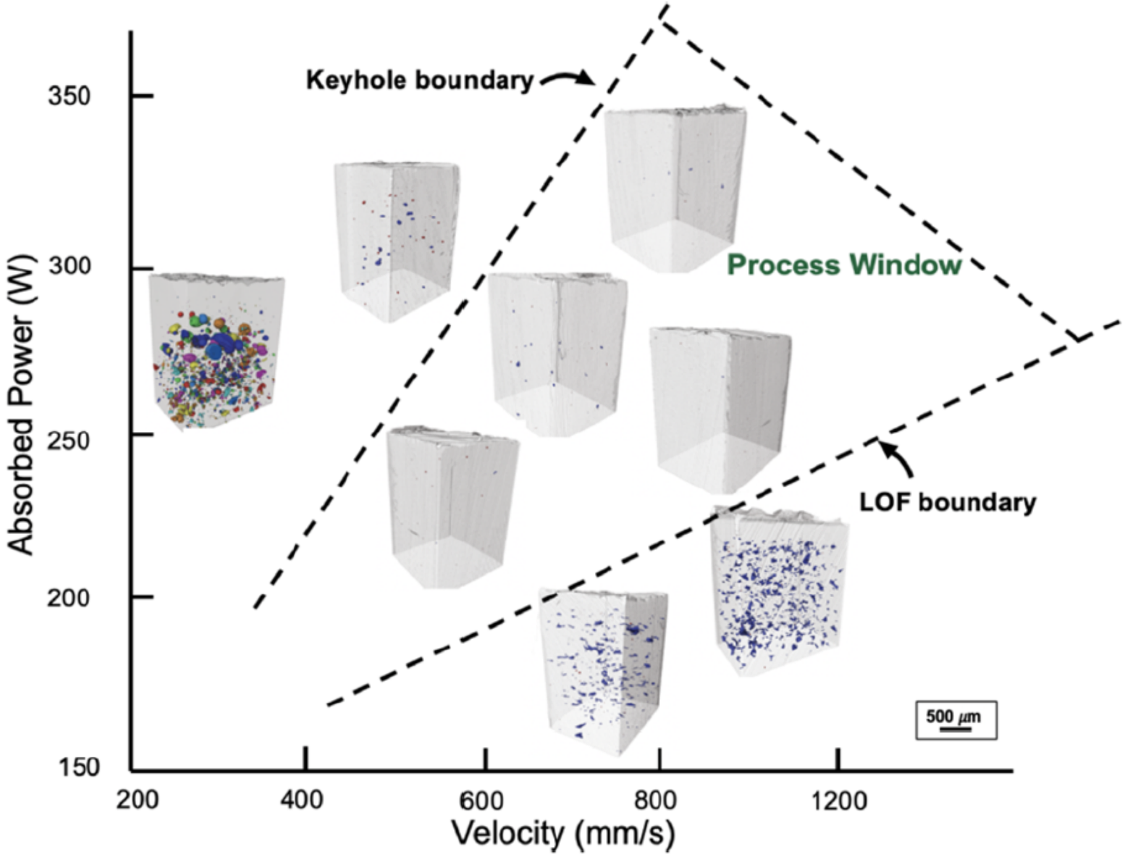

Variation of defect morphologies in TA64 alloy with respect to SLM process parameters. *[Gordon, Jerard V. et al., 2020, Additive Manufacturing]*

Literature Review

Fatigue behaviour

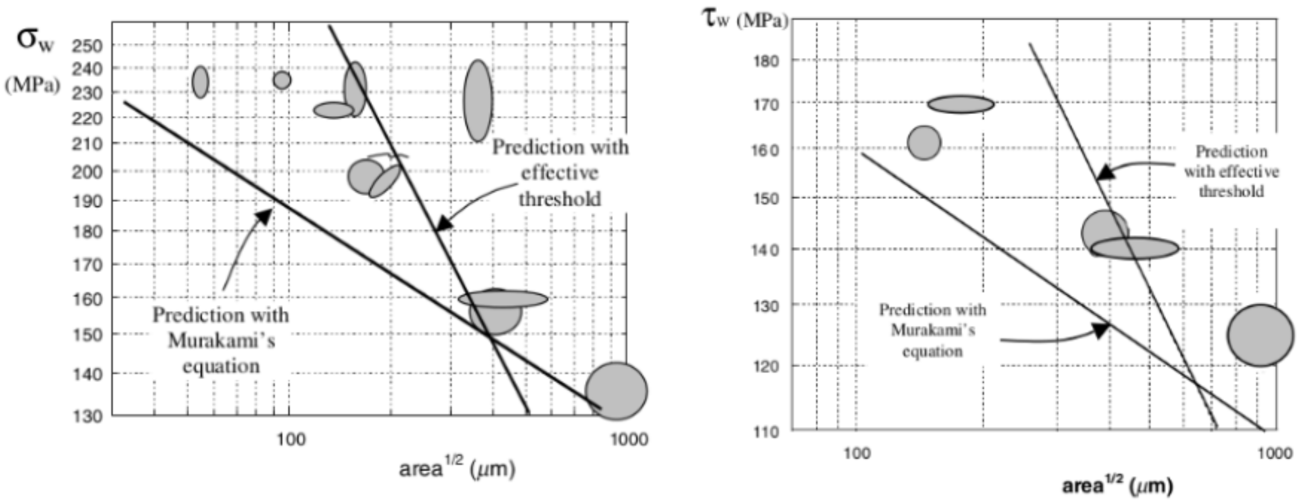

(left) Fully reversed tension/compression loading, variation of fatigue limit with $\sqrt{area}$ parameter. (right) Fully reversed torsion loading: evolution of the fatigue limit with $\sqrt{area}$. Material is C36 steel. *[Billaudeau, T., Y. Nadot, and G. Bezine, 2004, Acta Materialia]*

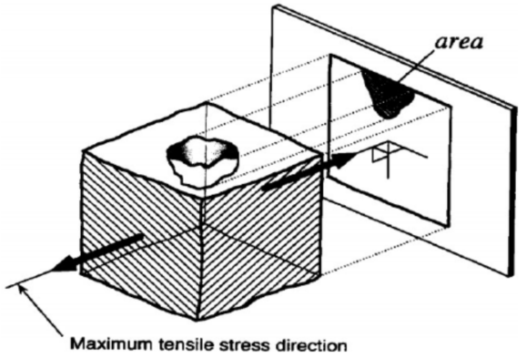

Murakami $\sqrt{area}$ parameter.

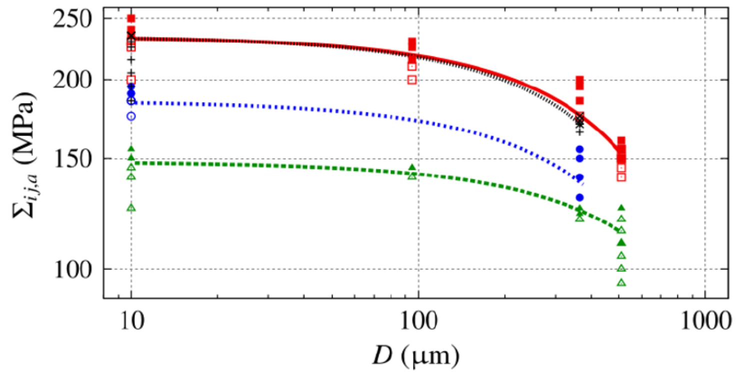

Loading condition	Tension	Torsion	Tension-torsion $\varphi = 45°$	Tension-torsion $\varphi = 90°$
Unbroken	⊡	△	⊙	+
Broken	■	▲	●	×

Fatigue test results at uniaxial and complex loading conditions, at R = -1. Material is SS 316L *[Guerchais, R. et al., 2015, Fatigue & Fracture of Engineering Materials & Structures]*

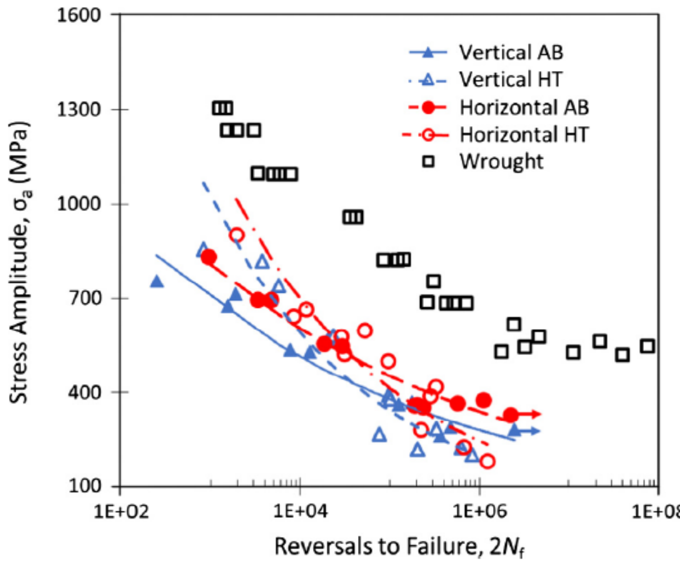

Strain-life fatigue data of SLM 17-4PH for different conditions. Note: where HT is CA-H900 condition. *[A. Yadollahi et al., Intl J. Fatigue, 2017]*

Literature Review

Intermediate conclusions

- ❑ Laser power (W) and scan speed (mm/s) are most influential parameters in the formation of gas pores and LoFs.
- ❑ In HCF regime, high-strength steels are more sensitive to defects.
- ❑ No significant influence of defect geometry under tensile and torsion loading condition (in C36 steel).
- ❑ There exists an influence of complex loading condition on the fatigue strength.

Global strategy

SLM process map study

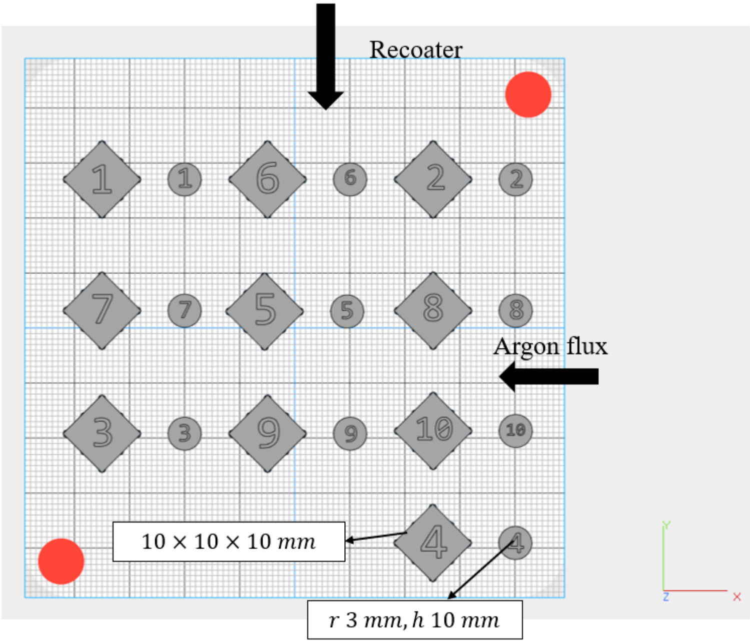

Fatigue tests

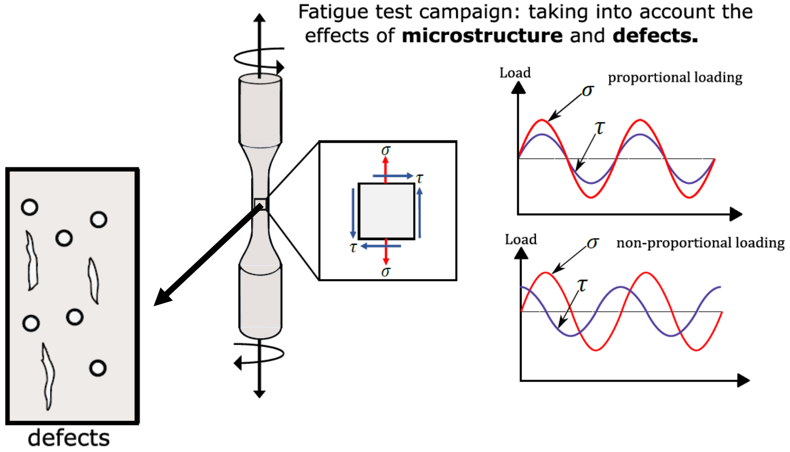

- Influence of defects anisotropy obtained from two different build orientation $\theta_1 and\ \theta_2$.
- Influence of complex loading conditions (in-phase, out-of-phase ($45^{\circ} or\ 90^{\circ}$) with different bi-axial stress ratios) in the presence of defects.

Numerical approach

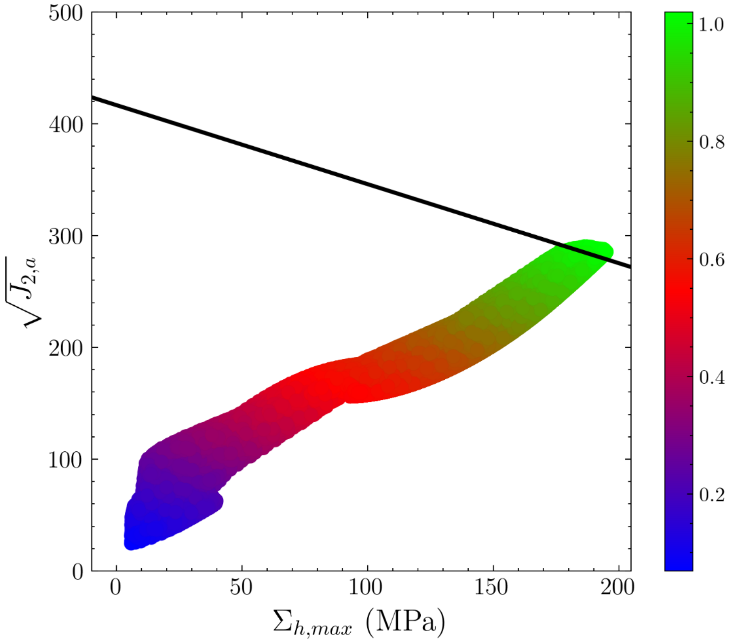

Microstructure and defect population control

- **SLM process map**

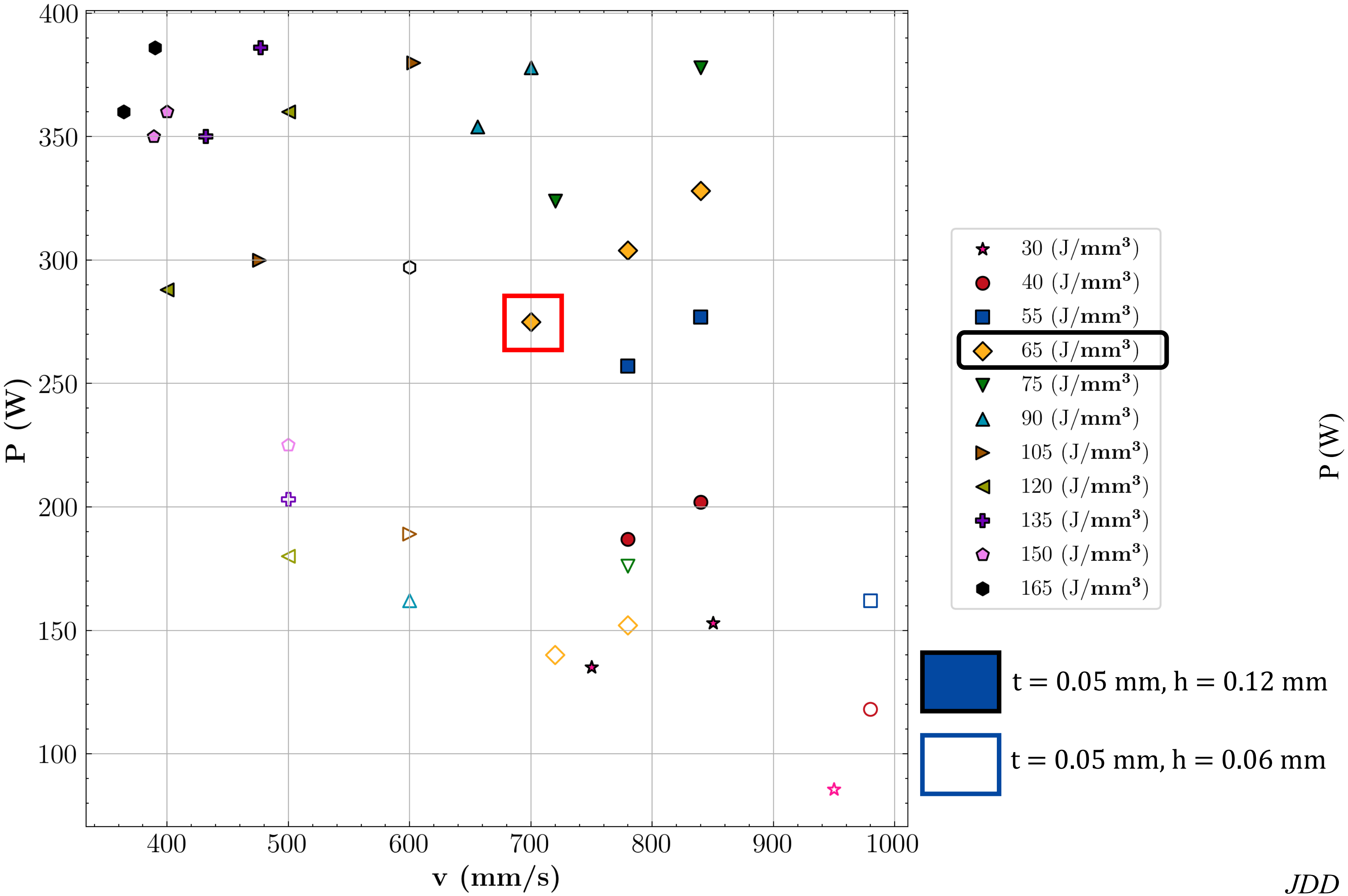

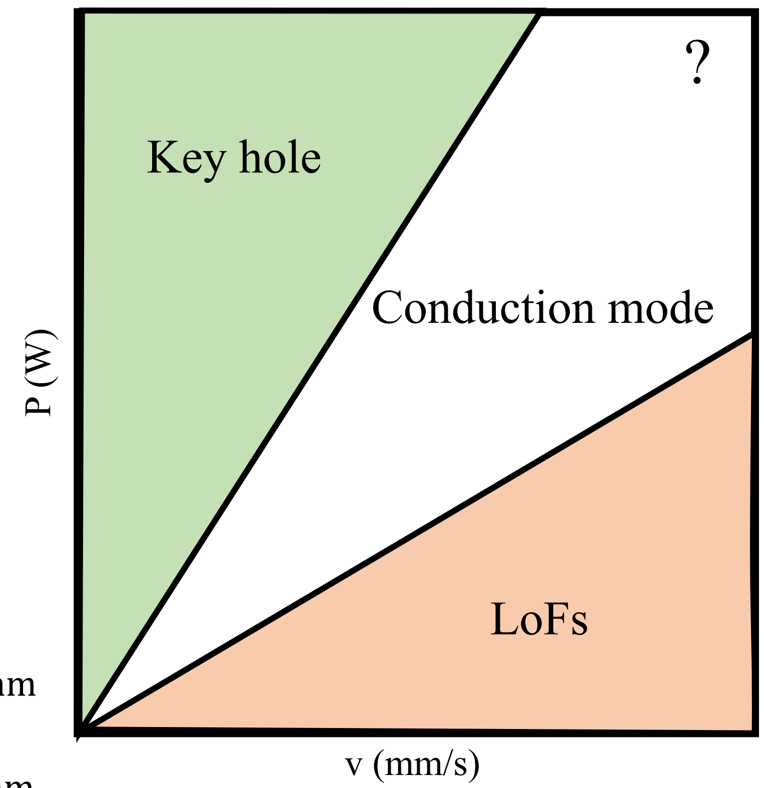

Microstructure and defect population control

- SLM process map

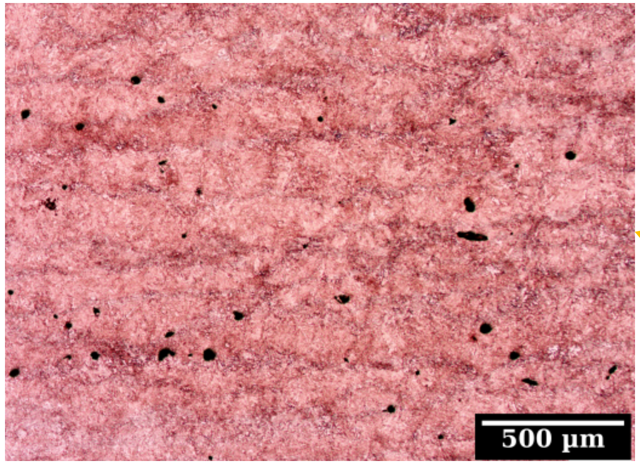

C30 165 J/mm³ HV 310

Microstructure

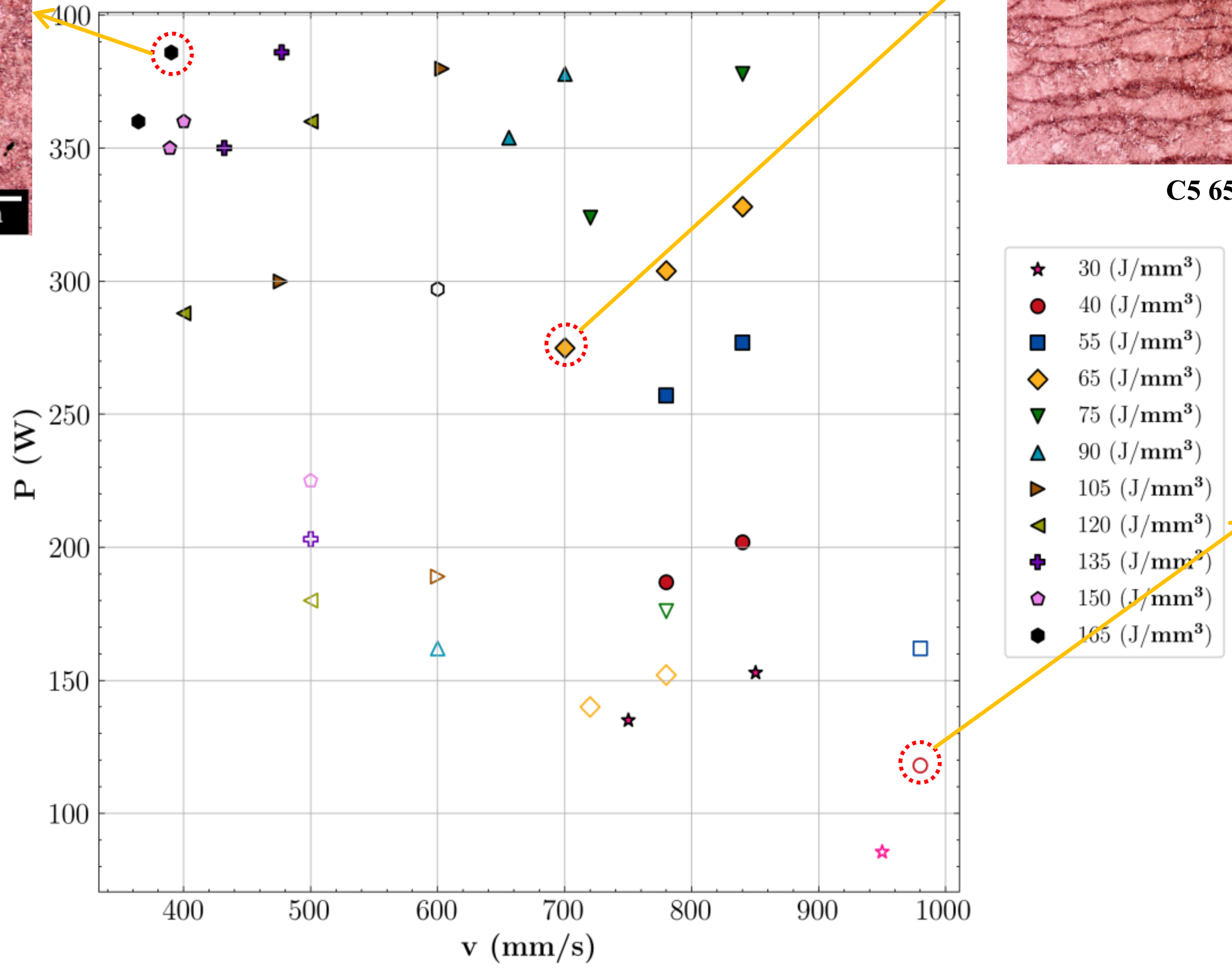

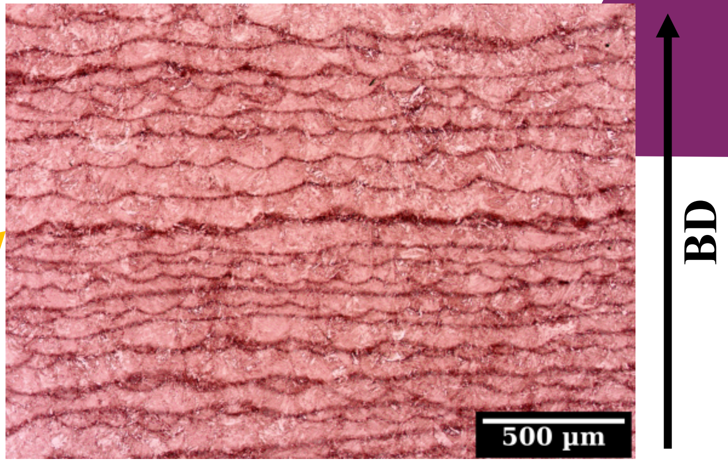

C5 65 J/mm³ (ideal) HV 355

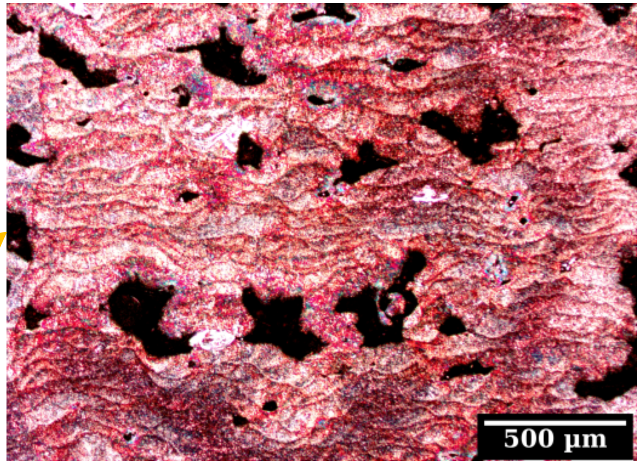

C8 40 J/mm³ HV 292

Arts et Métiers Sciences et Technologies

Microstructure and defect population control

- **SLM process map**

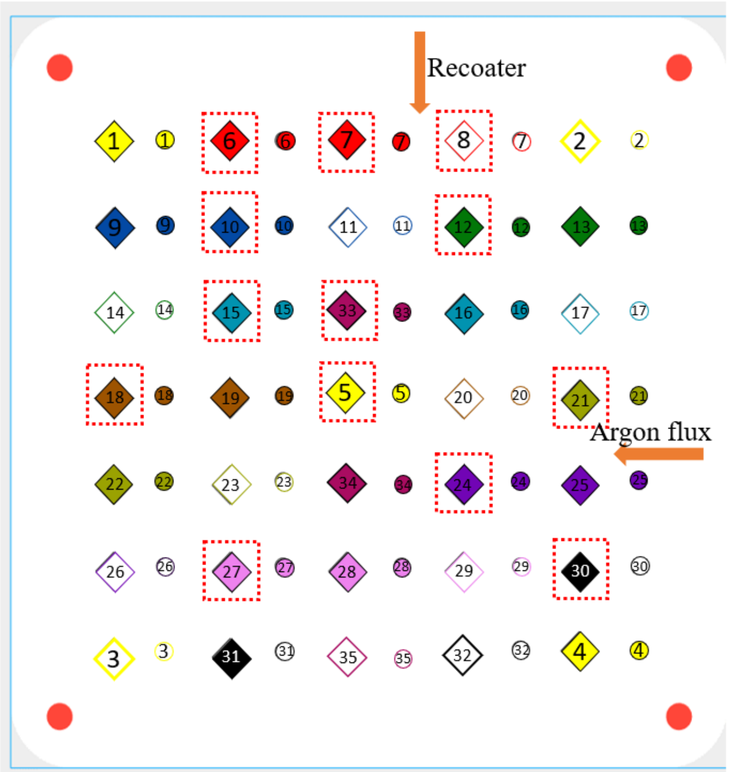

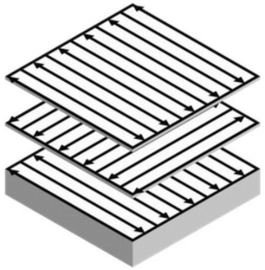

Stripes scan strategy

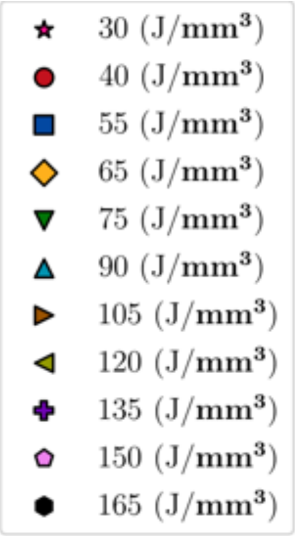

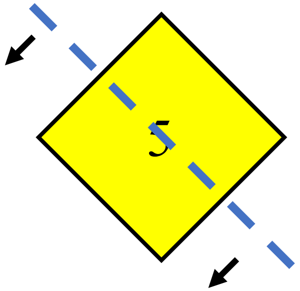

2D observations of defects

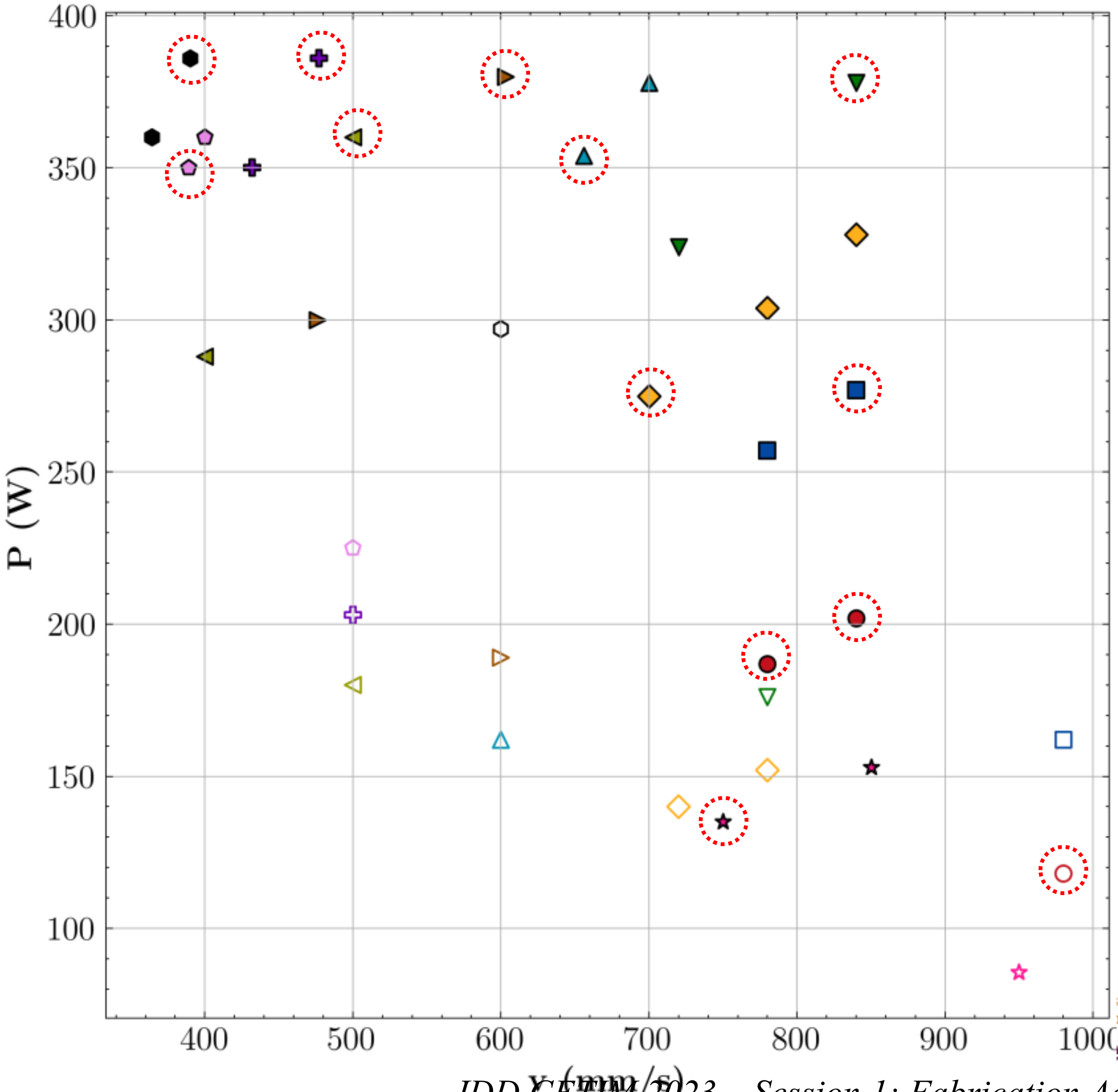

Microstructure and defect population control

- SLM process map

2D observations of defects

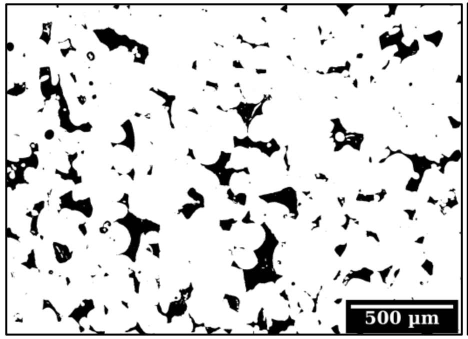

C33 30 J/mm³

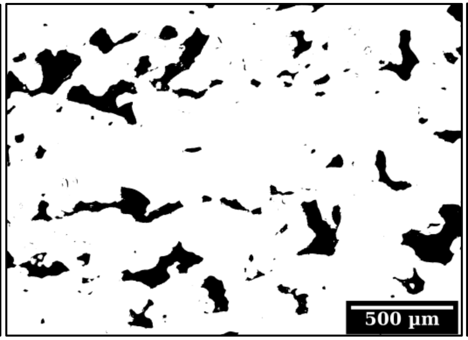

C8 40 J/mm³ h = 60µm

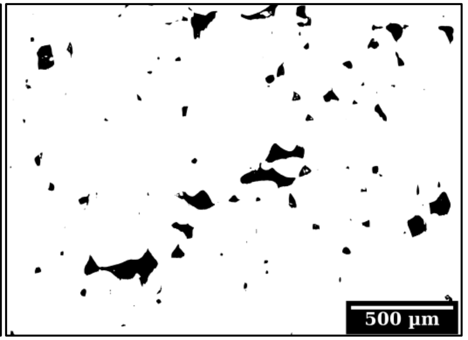

C6 40 J/mm³

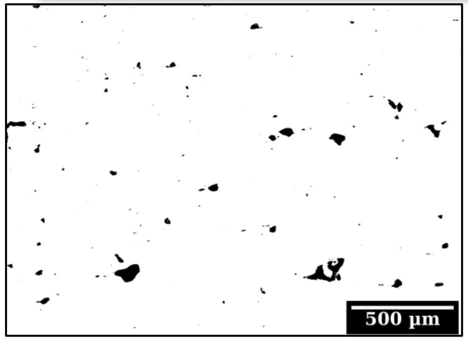

C7 40 J/mm³

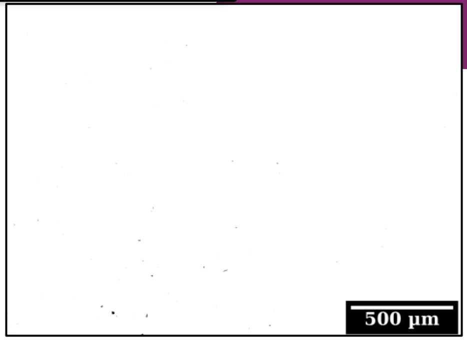

C10 55 J/mm³

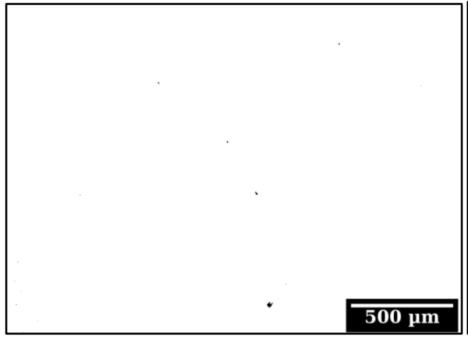

C5 65 J/mm³ (ideal)

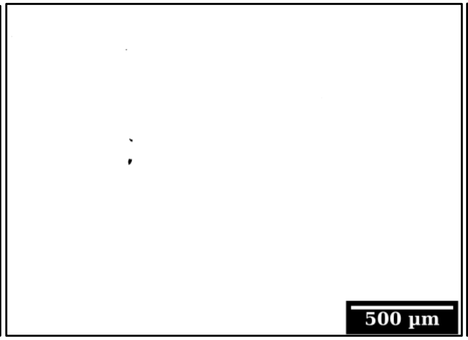

C12 75 J/mm³

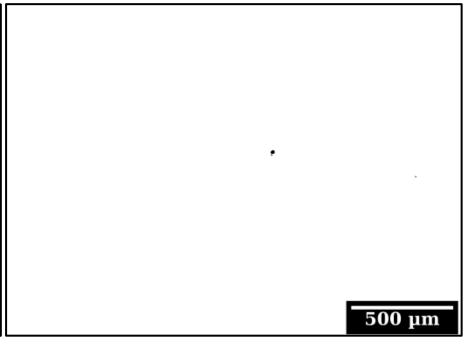

C15 90 J/mm³

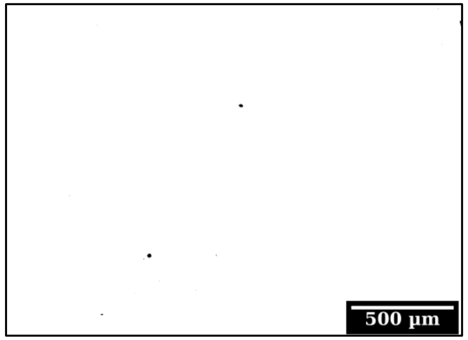

C18 105 J/mm³

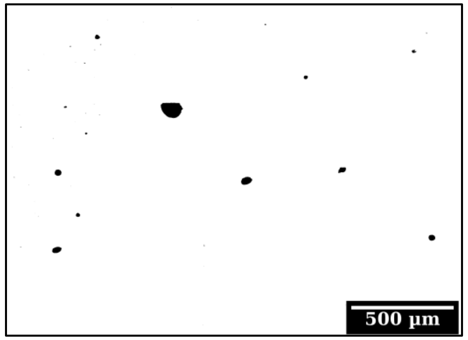

C21 120 J/mm³

BD

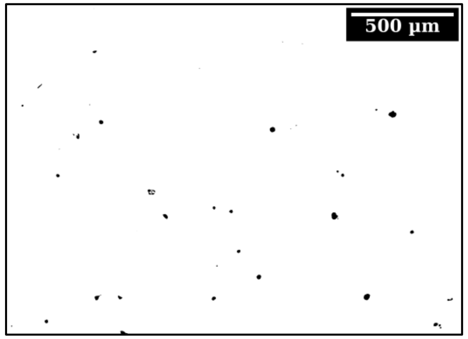

C24 135 J/mm³

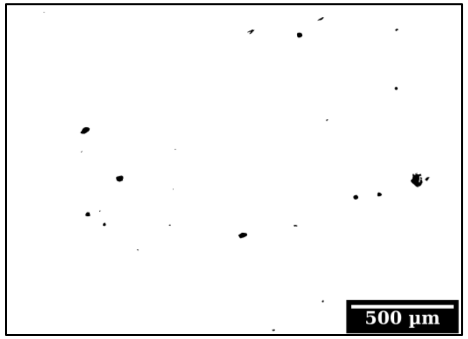

C27 150 J/mm³

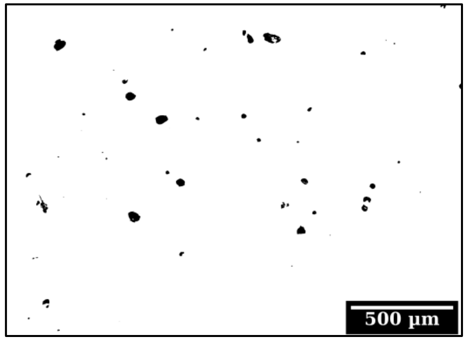

C30 165 J/mm³

Note: raw images are binarized

Arts Sciences et Technologies et Métiers

Statistical analysis of defects

- **2D observations**

Defect size as a function of circularity

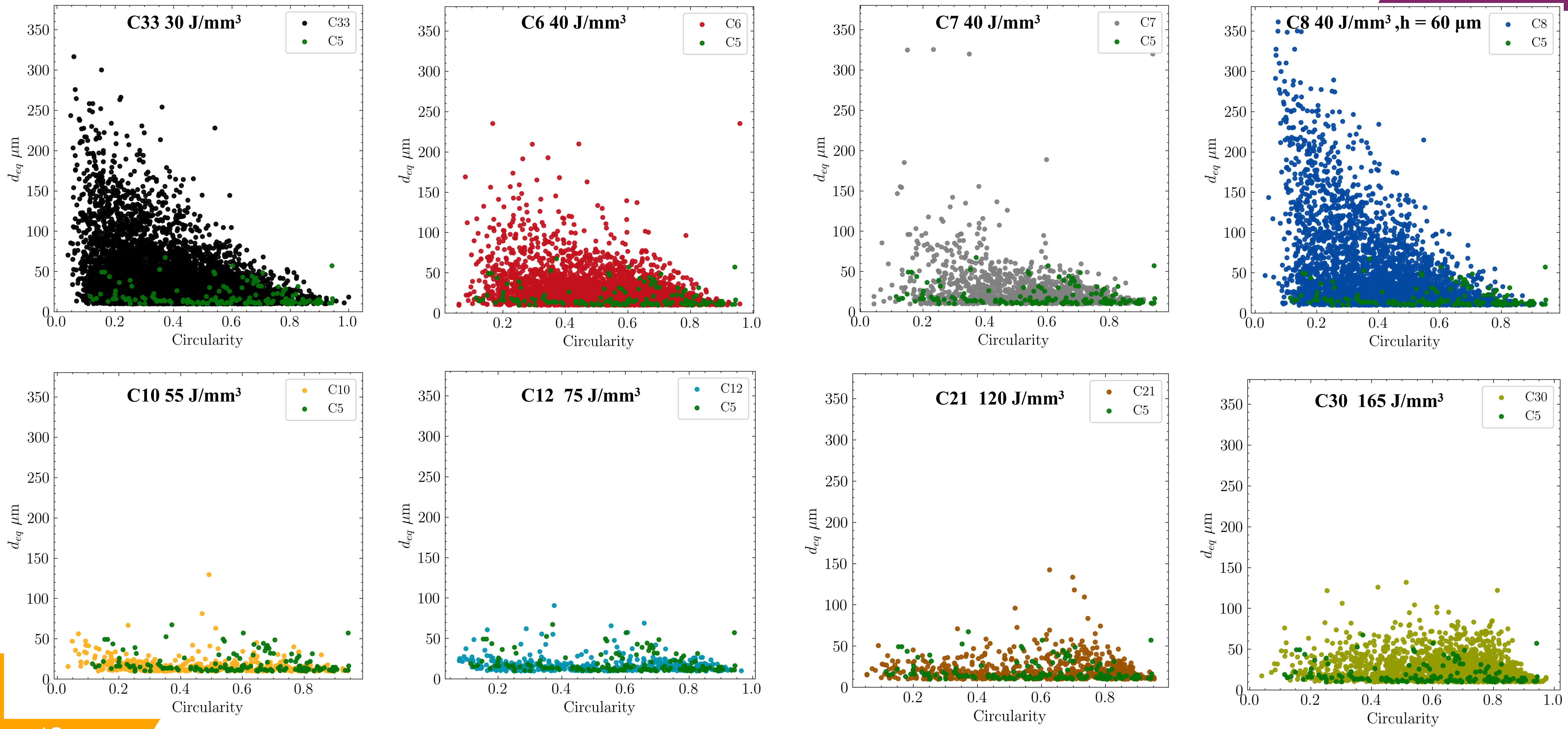

Statistical analysis of defects

- **2D observations**

Porosity (%) and defect density (defects/cm²)

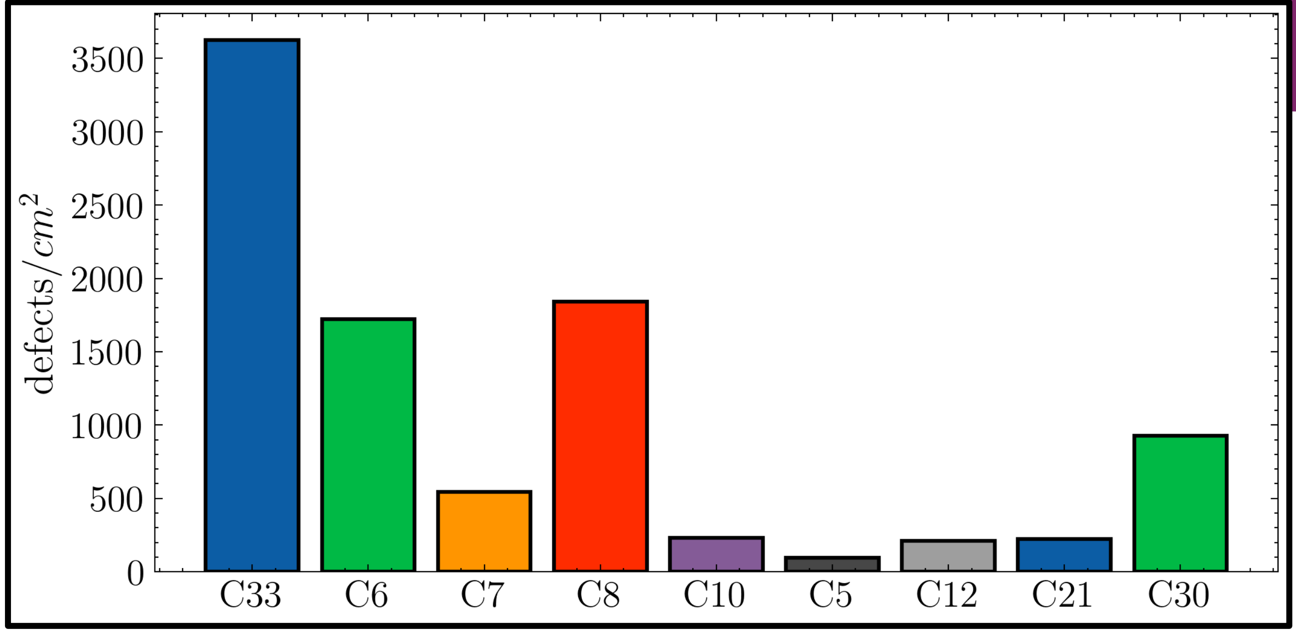

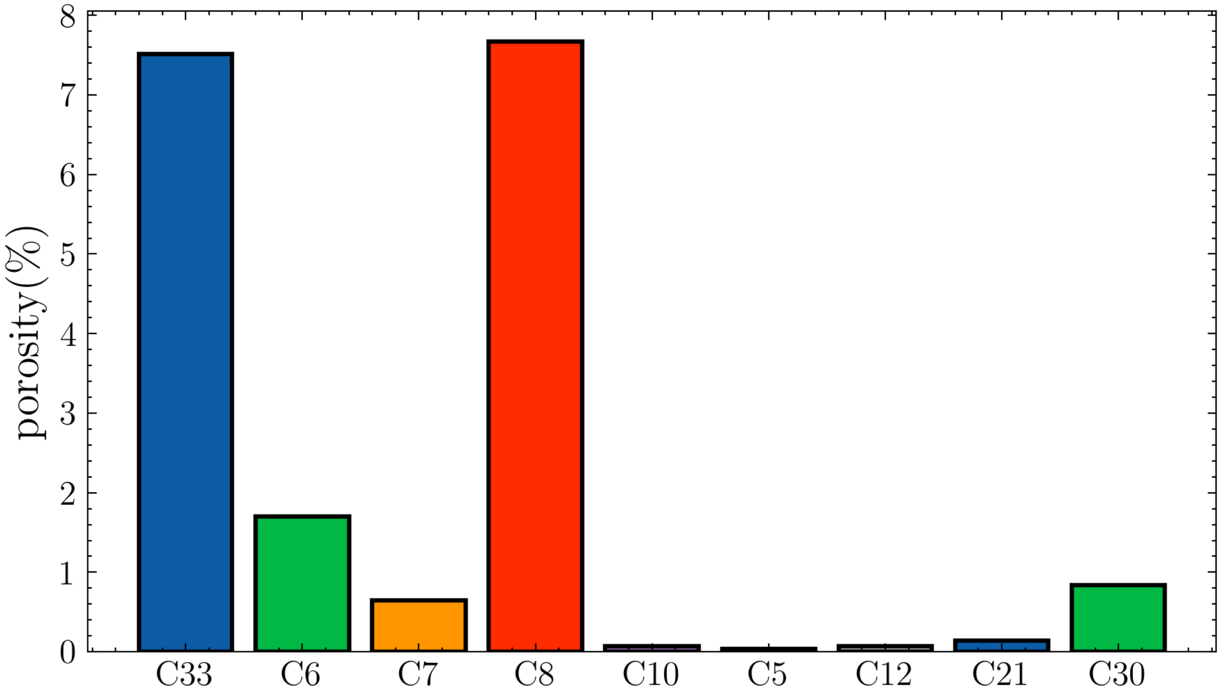

Note:

Specimen id	VED (J/mm³)
C33	30
C6	40
C7	40
C8	40 (h = 0.06 mm)
C10	55
C5	65
C12	75
C21	120
C30	165

Conclusions

- LoF zone at low energy density (between 30-40 J/mm^3) and key-hole mode at high energy densities (between 120 – 165 J/mm^3).
- High probability of finding a large defect in specimens fabricated at 30 and 40 J/mm^3.
- Presence of high number of complex shape defects whose circularity is between 0.1 to 0.6, in samples fabricated at 30 and 40 J/mm3.
- At 40 J/mm3, change in h (from 0.12 to 0.06 mm) has drastic outcomes in terms of porosity (%) and defect density (defects/cm^2).
- Sample C7 process parameters could be suitable for inducing LoFs in fatigue specimens.